Synthesis and characterization of white light emitting $Ca_xSr_{1-x}Al_2O_4:Tb^{3+},Eu^{3+}$ phosphor for solid state lighting

Samy K. K. Shaat,[1,2] Hendrik C. Swart,[1] and Odireleng M. Ntwaeaborwa[1,*]

[1]*Department of Physics, University of the Free State, Bloemfontein, ZA9300, South Africa*
[2]*Department of Physics, Islamic University, Gaza, P.O. Box 108, Gaza, Palestine*
**ntwaeab@ufs.ac.za*

Abstract: A white light emitting $Ca_xSr_{1-x}Al_2O_4:Tb^{3+};Eu^{3+}$ phosphor was synthesized by a combustion method using metal nitrates as precursors and urea as a fuel. The X-ray diffraction patterns from the samples showed phases associated with monoclinic structures of $CaAl_2O_4$ and $SrAl_2O_4$. White photoluminescence with the CIE coordinates (x = 0.343, y = 0.325) was observed when the phosphor was optically-excited at 227 nm using a monochromatized xenon lamp. The white photoluminescence was a result of the combination of blue and green line emissions from Tb^{3+}, and red line emission from Eu^{3+}. The structure and photoluminescence properties of this phosphor are reported.

OCIS codes: (160.4236) Nanomaterials; (160.5690) Rare-earth-doped materials; (250.5230) Photoluminescence.

References and links

1. Y. Song, G. Jia, M. Yang, Y. Huang, H. You, and H. Zhang, "$Sr_3Al_2O_5Cl_2:Ce^{3+},Eu^{2+}$: a potential tunable yellow-to-white-emitting phosphor for ultraviolet light emitting diodes," Appl. Phys. Lett. **94**(9), 091902 (2009).
2. J. S. Kim, P. E. Jeon, Y. H. Park, J. C. Choi, H. L. Park, G. C. Kim, and T. W. Kim, "White-light generation through ultraviolet-emitting diode and white-emitting phosphor," Appl. Phys. Lett. **85**(17), 3696–3698 (2004).
3. R. M. Farrell, E. C. Young, F. Wu, S. P. DenBaars, and J. S. Speck, "Materials and growth issues for high-performance nonpolar and semipolar light-emitting devices," Semicond. Sci. Technol. **27**(2), 024001 (2011).
4. H. Zhao, G. Liu, J. Zhang, J. D. Poplawsky, V. Dierolf, and N. Tansu, "Approaches for high internal quantum efficiency green InGaN light-emitting diodes with large overlap quantum wells," Opt. Express **19**(S4 Suppl 4), A991–A1007 (2011).
5. C. Wetzel and T. Detchprohm, "Wavelength-stable rare earth-free green light-emitting diodes for energy efficiency," Opt. Express **19**(S4 Suppl 4), A962–A971 (2011).
6. H. Zhao, G. Liu, and N. Tansu, "Analysis of InGaN-delta-InN quantum wells for light-emitting diodes," Appl. Phys. Lett. **97**(13), 131114 (2010).
7. J. Zhang and N. Tansu, "Improvement in spontaneous emission rates for InGaN quantum wells on ternary InGaN substrate for light-emitting diodes," J. Appl. Phys. **110**(11), 113110 (2011).
8. T. Akasaka, H. Gotoh, Y. Kobayashi, and H. Yamamoto, "Extremely narrow violet photoluminescence line from ultrathin InN single quantum well on step-free GaN surface," Adv. Mater., doi:10.1002/adma.201200871.
9. J. Zhang, H. Zhao, and N. Tansu, "Effect of crystal-field split-off hole and heavy-hole bands crossover on gain characteristics of high Al-content AlGaN quantum well lasers," Appl. Phys. Lett. **97**(11), 111105 (2010).
10. J. Zhang, H. Zhao, and N. Tansu, "Large optical gain AlGaN-delta-GaN quantum wells laser active regions in mid- and deep-ultraviolet spectral regimes," Appl. Phys. Lett. **98**(17), 171111 (2011).
11. Y. Taniyasu and M. Kasu, "Polarization property of deep-ultraviolet light emission from C-plane AlN/GaN short-period superlattices," Appl. Phys. Lett. **99**(25), 251112 (2011).
12. E. Francesco Pecora, W. Zhang, A. Yu. Nikiforov, L. Zhou, D. J. Smith, J. Yin, R. Paiella, L. Dal Negro, and T. D. Moustakas, "Sub-250 nm room-temperature optical gain from AlGaN/AlN multiple quantum wells with strong band-structure potential fluctuations," Appl. Phys. Lett. **100**(6), 061111 (2012).
13. X. Rao, Q. Huang, X. Yang, Y. Cui, Y. Yang, C. Wu, B. Chen, and G. Qian, "Color tunable and white light emitting Tb^{3+} and Eu^{3+} doped lanthanide metal–organic framework materials," J. Mater. Chem. **22**(7), 3210–3214 (2012).
14. H.-C. Kuo, C.-W. Hung, H.-C. Chen, K.-J. Chen, C.-H. Wang, C.-W. Sher, C.-C. Yeh, C.-C. Lin, C.-H. Chen, and Y.-J. Cheng, "Patterned structure of remote phosphor for phosphor-converted white LEDs," Opt. Express **19**(S4 Suppl 4), A930–A936 (2011).

#169669 - $15.00 USD Received 1 Jun 2012; revised 17 Jun 2012; accepted 20 Jun 2012; published 21 Jun 2012

15. C. Liu, Y. Wang, Y. Hu, R. Chen, and F. Liao, "Adjusting luminescence properties of $Sr_xCa_{1-x}Al_2O_4:Eu^{2+}$, Dy^{3+} phosphors by Sr/Ca ratio," J. Alloy. Comp. **470**(1-2), 473–476 (2009).
16. S. H. Ju, S. G. Kim, J. C. Choi, H. L. Park, S.-I. Mho, and T. W. Kim, "Determination of the solid solubility of $SrAl_2O_4$ in $CaAl_2O_4$ through crystal field-dependent Eu^{2+} signatures," Mater. Res. Bull. **34**(12-13), 1905–1909 (1999).
17. D. Geng, G. Li, M. Shang, C. Peng, Y. Zhang, Z. Cheng, and J. Lin, "Nanocrystalline $CaYAlO_4:Tb^{3+}/Eu^{3+}$ as promising phosphors for full-color field emission displays," Dalton Trans. **41**(10), 3078–3086 (2012).
18. R. Martínez-Martínez, E. Álvarez, A. Speghini, C. Falcony, and U. Caldiño, "Cold white light generation from hafnium oxide films activated with Ce^{3+}, Tb^{3+}, and Mn^{2+} ions," J. Mater. Res. **25**(03), 484–490 (2010).
19. D. Wang, P. Yang, Z. Cheng, W. Wang, Z. Hou, Y. Dai, C. Li, and J. Lin, "Patterning of $Gd_2(WO_4)_3:Ln^{3+}$ (Ln=Eu, Tb) luminescent films by microcontact printing route," J. Colloid Interface Sci. **365**(1), 320–325 (2012).
20. A. Potdevin, G. Chadeyron, D. Boyer, B. Caillier, and R. Mahiou, "Sol–gel based YAG:Tb^{3+} or Eu^{3+} phosphors for application in lighting sources," J. Phys. D. **38**(17), 3251–3260 (2005).
21. P. Zhu, Q. Zhu, H. Zhu, H. Zhao, B. Chen, Y. Zhang, X. Wang, and W. Di, "Effect of SiO_2 coating on photoluminescence and thermal stability of $BaMgAl_{10}O_{17}$: Eu^{2+} under VUV and UV excitation," Opt. Mater. **30**(6), 930–934 (2008).
22. S. Fan, C. Yu, D. He, X. Wang, and L. Hu, "Tunable white light emission from γ-irradiated Ag/Eu co-doped phosphate glass phosphor," Opt. Mater. Express **2**(6), 765–770 (2012).

1. Introduction

Today, many researchers are making efforts to develop white light emitting phosphors that can be used in solid state lighting applications such as phosphor lamps and light emitting diodes (LEDs). In traditional white light LEDs, white light is generated by combining a lnGaN-based blue diode with a yellow phosphor such as YAG:Ce^{3+} or by combining a UV chip with a three converter system of red, green and blue phosphors. However, YAG:Ce^{3+} has been reported to show high thermal quenching and poor colour rendition. In addition, the blue emission efficiency is often affected by re-absorption by the red or green phosphor in the three converter system [1]. One way of addressing these inefficiencies is to develop a single phosphor that emits white light constituted by simultaneous emission of blue, green, and red light when excited by ultraviolet (UV) radiation. For example, Kim et al. [2] were able to generate white light from $Sr_3MgSi_2O_8:Eu^{2+},Mn^{2+}$ based on broadband emissions with maxima at 470, 570 and 680 nm while Song et al. [1] reported white light from a tunable $Sr_3Al_2O_5Cl_2:Ce^{3+},Eu^{2+}$ based on energy transfer from Ce^{3+} to Eu^{2+} by a down-conversion process. It has been demonstrated that the development of white LEDs depends on the advances in the visible InGaN-based LEDs [3–8], which are key technologies for pump excitation for white LEDs. The advances in nitride LEDs have also led to high-performance sources emitting in the green spectral regimes [3–5], and several approaches based on novel QWs have also been used to extend the emission wavelengths to yellow/red spectral regimes [6–8]. Specifically, related to the development of LEDs-based pump sources applicable for the current white phosphor discussed here, the importance of having high performance deep UV LEDs [9–12] is of great importance for enabling the proposed white light-emitting phosphor material to be practical. Recently, significant works have been pursued to achieve improved understanding on the physics of high Al-content AlGaN quantum wells [9–12] for achieving high performance deep- and mid-UV LEDs/lasers, which will be applicable as pump excitation source for the white phosphor. In this study, white photoluminescence was observed from $Ca_xSr_{1-x}Al_2O_4:Tb^{3+},Eu^{3+}$ phosphor that was prepared by the combustion method. The white photoluminescence was a result of the simultaneous emission of blue and green light from Tb^{3+}, and red light from Eu^{3+} when the phosphor was excited at 227 nm using a monochromatized xenon lamp. This result is unique because the generated white was a combination of blue, green and red narrow line emissions compared to broadband (or a combination of broadband and narrow line) emissions reported from a variety of phosphors used in white LEDs [13–15]. Furthermore, the blue, green and red line emissions occurred simultaneously following excitation by photons of sufficiently high energy rather than by a UV down-conversion process, i.e. capturing of the UV excitation energy by one luminescent centre and a subsequent transfer to the other luminescent centre as reported in ref [13]. This

#169669 - $15.00 USD Received 1 Jun 2012; revised 17 Jun 2012; accepted 20 Jun 2012; published 21 Jun 2012

phosphor is evaluated for a possible application as a source of white light in solid state lighting devices.

2. Experiments

$Ca_xSr_{1-x}Al_2O_4:Tb^{3+},Eu^{3+}$ (x = 0, 1, 0.3 and 0.7) phosphors were prepared by a combustion method. In a typical preparation, stoichiometric amounts of metal nitrates: $Ca(NO_3)_2.4H_2O$, $Sr(NO_3)_2$, $Al(NO_3)_3.9H_2O$, $Tb(NO_3)_3.6H_2O$ and $Eu(NO_3)_3.5H_2O$; and urea ($CO(NH_2)_2$) were mixed and dissolved in distilled water. A homogeneous solution was obtained after stirring vigorously for 20 minutes. The solution was transferred to a muffle furnace pre-heated to and maintained at a temperature of 500 ± 10°C. After all the liquid had evaporated, the reagents decomposed and released large amounts of gases. A large amount of heat released (due to the exothermic nature of this process) resulted in a flame that decomposed the reagents further and released more gases. The flame lasted for ~60 seconds and the combustion process was completed within 5 minutes. The resulting combustion products (powders) were cooled down to room temperature and were ground gently using a pestle and mortar.

$Ca_xSr_{1-x}Al_2O_4:Tb^{3+},Eu^{3+}$ (x = 0, 1, 0.3 and 0.7) phosphors with different concentrations of Ca^{2+} and Sr^{2+} were produced. The concentration of Tb^{3+} and Eu^{3+} were fixed at 0.6 and 0.4 mol% respectively in all samples. The powders were characterized without any further post-preparation treatment. The crystalline structure of the phosphor was analyzed using a Bruker D8 Advanced powder diffractometer and the photoluminescence (excitation and emission) data were recorded using a Cary Eclipse fluorescence spectrophotometer.

3. Results and discussions

Figure 1 shows the X –ray diffraction (XRD) patterns of $Ca_xSr_{1-x}Al_2O_4:Tb^{3+},Eu^{3+}$ (x = 0, 0.3, 1 and 0.7). For x = 0, the patterns are consistent with the standard monoclinic structure of $SrAl_2O_4$ referenced in JCPDS file No. 70-134. Except for a marginal increase in the diffraction peak intensities, this structure did not change when x = 0.3. For x = 1, the patterns resembles the standard monoclinic structure of $CaAl_2O_4$ referenced in JCPDS file No. 34-379. When x = 0.7, the $\bar{2}20$ peak shifted slightly to the left. The shifting can be attributed to the expansion of the $CaAl_2O_4$ crystal lattice due to the substitution of Ca^{2+} by Sr^{2+} whose ionic radius (0.123 nm) is greater than that of Ca^{2+} (0.114 nm) [16,17]. The Tb^{3+} and Eu^{3+} ions with ionic radii of 0.109 nm and 0.112 nm [18] respectively had no effect on the crystalline structure of the host due to their relatively lower concentrations. These ions are expected to preferentially occupy the Ca^{2+} and Sr^{2+} sites due to similarities in their ionic radii. The average particle size of the phosphors estimated using the Debye-Scherrer equation was ~30 nm.

#169669 - $15.00 USD Received 1 Jun 2012; revised 17 Jun 2012; accepted 20 Jun 2012; published 21 Jun 2012

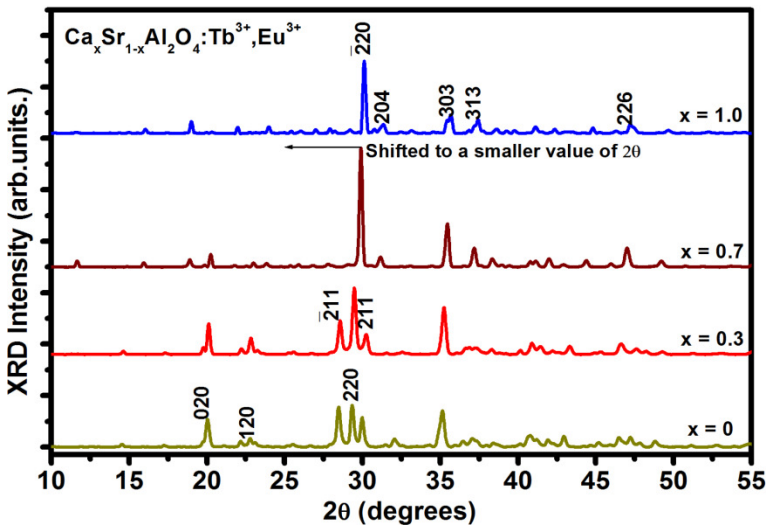

Fig. 1. XRD spectra of $Ca_xSr_{1-x}Al_2O_4:Tb^{3+},Eu^{3+}$ phosphors with x = 0, 0.3, 0.7, and 1.

The photoluminescence (PL) excitation and emission spectra were recorded from all $Ca_xSr_{1-x}Al_2O_4:Tb^{3+},Eu^{3+}$ powders with x = 0, 0.3, 0.7, and 1; but white light was only observed from the powder with x = 0.3. Therefore we present only the spectra recorded from the powder with x = 0.3. Figure 2 shows the photoluminescence (PL) excitation spectrum of Ca_xSr_{1-x} $Al_2O_4:Tb^{3+},Eu^{3+}$ recorded when monitoring major emission peaks at 380, 416, 437 and 543 nm, all coming from Tb^{3+}; and at 617 nm coming from Eu^{3+}. The excitations peaking at ~227 nm are assigned to direct excitation of Tb^{3+}through f→d transitions while the excitation peak at 240 nm is assigned to $Eu^{3+}\rightarrow O^{2-}$ charge transfer transitions resulting from transfer of electrons from O^{2-} ($2p^6$) orbitals to the $4f^7$ and $4f^6$ states of Eu^{3+} respectively. These transitions are assigned according to the literature cited [19,20].

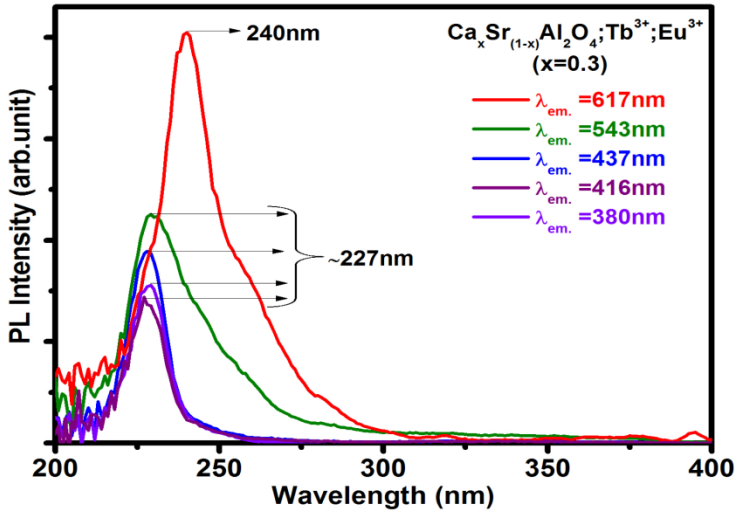

Fig. 2. PL excitation spectra of $Ca_xSr_{1-x}Al_2O_4:Tb^{3+},Eu^{3+}$ phosphor.

Figure 3 shows the PL emission spectra of $Ca_xSr_{1-x}Al_2O_4$: Tb^{3+},Eu^{3+} phosphor recorded when the phosphors were excited at 240 nm. The insets are the PL emission spectra of Ca_xSr_{1-x} $Al_2O_4:Tb^{3+}$ and $Ca_xSr_{1-x}Al_2O_4:Eu^{3+}$ phosphors also recorded when the phosphors were excited at 240 nm. As shown in the one inset, the emission spectrum of $Ca_xSr_{1-x}Al_2O_4:Tb^{3+}$

#169669 - $15.00 USD Received 1 Jun 2012; revised 17 Jun 2012; accepted 20 Jun 2012; published 21 Jun 2012

consists of major green emission at 543 nm ascribed to the $^5D_4 \rightarrow {}^7F_5$ transition of Tb^{3+} and minor emission peaks at 380 (violet), 416 (blue), 437 (blue) ascribed to the $^5D_3 \rightarrow {}^7F_J$ (J = 6, 5, 4) transitions of Tb^{3+} and 484 nm (bluish-green) ascribed to the transitions of $^5D_4 \rightarrow {}^7F_6$ transition of Tb^{3+}. In the other inset, the PL emission spectrum of $Ca_xSr_{1-x}Al_2O_4:Eu^{3+}$ consists of major red emission at 617 nm (red) ascribed to the $^5D_0 \rightarrow {}^7F_2$ transition of Eu^{3+} and minor emissions at 590, 653 and 702 nm ascribed to the $^5D_0 \rightarrow {}^7F_J$ (J = 1, 3, 4) transitions of Eu^{3+}. The PL emission spectrum of Ca_xSr_{1-x} $Al_2O_4:Tb^3,Eu^{3+}$ consists of emission peaks from both Eu^{3+} and Tb^{3+} with major emissions at 617 nm coming from Eu^{3+}. Notice that all the Tb^{3+} peaks in Fig. 4 resemble those observed from $Ca_xSr_{1-x}Al_2O_4:Tb^{3+}$ in the inset. In the same manner, the Eu^{3+} emission peaks resemble those observed from $Ca_xSr_{1-x}Al_2O_4:Eu^{3+}$ in the other inset. That is, the PL emission spectra of Ca_xSr_{1-x} $Al_2O_4:Tb^{3+},Eu^{3+}$ is a combination of the spectra shown in the two insets suggesting that there was no energy transfer between Tb^{3+} and Eu^{3+}. It is therefore most likely that in this particular host the f→d transitions of Tb^{3+} and $O^{2-} \rightarrow Eu^{3+}$ charge transfer transitions occurred simultaneously following excitation by photons of sufficiently high energy.

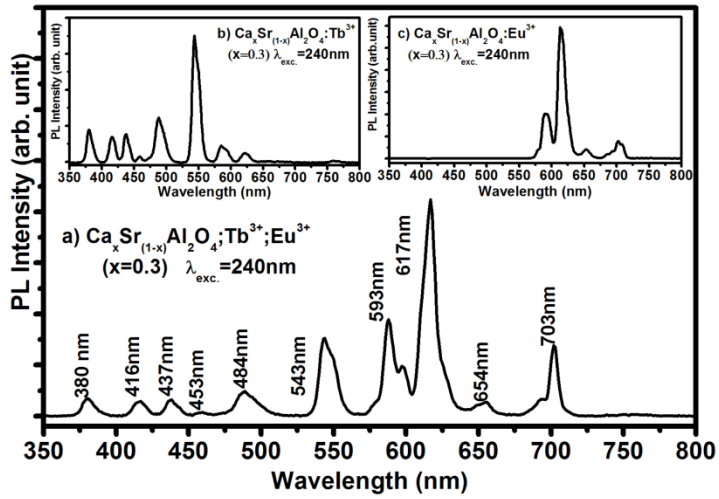

Fig. 3. PL emission spectra of $Ca_xSr_{1-x}Al_2O_4:Tb^{3+};Eu^{3+}$. The insets are the PL emission spectra of $Ca_xSr_{1-x}Al_2O_4:Tb^{3+}$ and $Ca_xSr_{1-x}Al_2O_4:Eu^{3+}$. All the phosphors were excited at 240 nm.

Figure 4 shows the PL emission spectra of Ca_xSr_{1-x} $Al_2O_4:Tb^{3+},Eu^{3+}$ phosphor recorded when the phosphor was excited at 227 nm. The insets are the emission spectra of Ca_xSr_{1-x} $Al_2O_4:Tb^{3+}$ and $Ca_xSr_{1-x}Al_2O_4:Eu^{3+}$ (x = 0.3) also recorded when the phosphors were excited at 227 nm. The emission spectrum of the Ca_xSr_{1-x} $Al_2O_4:Eu^{3+}$ in inset of Fig. 4 is the same as that observed when the same sample was excited at 240 nm as shown in the inset of Fig. 3. The emission spectrum of $Ca_xSr_{1-x}Al_2O_4:Tb^{3+}$ (in the other inset) consists of four major line emission peaks with maxima at 380, 416, 437 ascribed to the $^5D_3 \rightarrow {}^7F_J$ (J = 6,5,4) transition of Tb^{3+} and 543 nm ascribed to the $^5D_4 \rightarrow {}^7F_5$ transition of Tb^{3+}. Notice that the violet-blue line emissions at 380, 416, 437 nm are more intense than the well known green emission from Tb^{3+} at 543 nm, which is the opposite of the peak intensities of the same sample in the inset of Fig. 3. The increase in the intensity of the blue emission due to the $^5D_3 \rightarrow {}^7F_J$ of Tb^{3+} (compared to the well known green emission due to $^5D_4 \rightarrow {}^7F_5$ transitions) has been reported to be due to suppressed cross relaxation (non-radiative transitions) from the $^5D_3$ to $^5D_4$ state at relatively lower concentrations (<< 1 mol%) of Tb^{3+} [18,21]. At higher concentrations (>> 1 mol%) of Tb^{3+}, the well known green emission due to $^5D_4 \rightarrow {}^7F_5$ has been found to be much more intense than all other Tb^{3+} emissions. Consistent with these reports, we observed increased blue emission due to the $^5D_3 \rightarrow {}^7F_J$ transitions at a relatively lower

#169669 - $15.00 USD Received 1 Jun 2012; revised 17 Jun 2012; accepted 20 Jun 2012; published 21 Jun 2012

concentration (0.6 mol%) of Tb^{3+}. In addition, we observed increased blue emission from 0.6 mol% of Tb^{3+} in $CaAl_2O_4:Tb^{3+}$ while the green emission was prominent in $SrAl_2O_4:Tb^{3+}$ (PL spectra not shown), suggesting that $^5D_3 \rightarrow {}^7F_J$ transitions are preferentially favoured when Tb^{3+} ions occupy Ca^{2+} sites than Sr^{2+} sites. Zhu et al [22] have demonstrated that Eu^{2+} can occupy three different sites in SiO_2 coated $BaMgAl_{10}O_{17}$ giving different emission intensities when excited at different wavelengths. It is therefore most likely that in our $Ca_xSr_{1-x}Al_2O_4:Tb^{3+},Eu^{3+}$ system, the blue emission was mainly due to Tb^{3+} ions occupying the Ca^{2+} sites while the green emission was mainly coming from those occupying the Sr^{2+} sites. On the other hand, the red emission from Eu^{3+} at 617 nm was consistent and was not dependent on whether or not Eu^{3+} ions occupy the Ca^{2+} or Sr^{2+} sites. In order to balance the blue, green and red emissions, the relative intensities of these emissions were tuned by adjusting the mol ratio of Ca^{2+} to Sr^{2+} and the right combination was found to be 0.3:0.7 (i.e. when x = 0.3). The reason why the balance was obtained when x = 0.3 is not known yet but this study is in progress and our findings will be reported in future publications. As shown in Fig. 4, the PL emission spectrum of Ca_xSr_{1-x} $Al_2O_4:Tb^{3+},Eu^{3+}$ consists of blue and green line emissions from Tb^{3+} and red line emissions from Eu^{3+} and their combination constituted white light. Notice that all the Tb^{3+} and Eu^{3+} peaks in Fig. 4 resemble the peaks observed when $Ca_xSr_{1-x}Al_2O_4:Tb^{3+}$ and $Ca_xSr_{1-x}Al_2O_4:Eu^{3+}$ were excited at 227 nm as shown in the insets except that the 543 nm peak is marginally more intense than all other peaks. Again, these emissions are most probably a result of simultaneous occurrence of $f \rightarrow d$ and $O^{2-} \rightarrow Eu^{3+}$ charge transfer transitions after excitation by photons of sufficiently high energy and a subsequent emission of blue, green and red photons. After testing different phosphors with different mol ratios of $Ca^{2+}:Sr^{2+}$ we concluded that there are two important conditions to produce white photoluminescence from our material, namely the mol ratio of $Ca^{2+}:Sr^{2+}$ and the excitation wavelength. For example, we were only able to produce white light when we excited Ca_xSr_{1-x} $Al_2O_4:Tb^{3+},Eu^{3+}$ at 227 nm when the mol ratio of Ca^{2+} to Sr^{2+} was 0.3:0.7. This is probably due to the fact the $f \rightarrow d$ direct excitation of Tb^{3+} and the $O^{2-} \rightarrow Eu^{3+}$ charge transfer are overlapping at this wavelength.

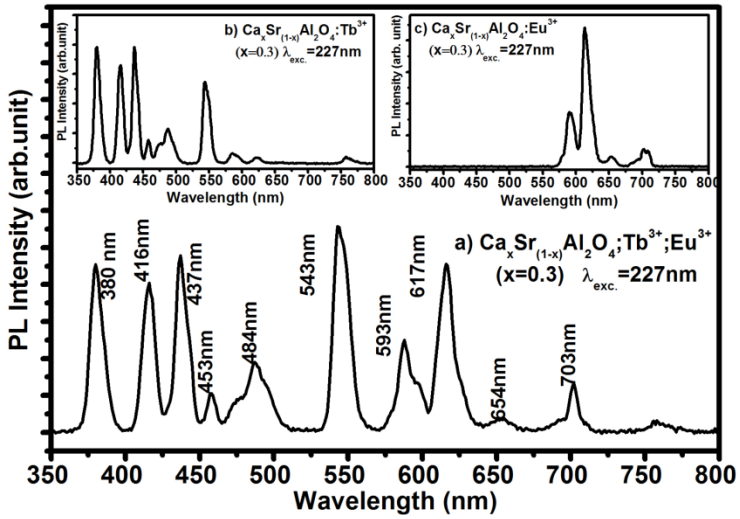

Fig. 4. PL emission spectra of $Ca_xSr_{1-x}Al_2O_4:Tb^{3+},Eu^{3+}$. The insets are the PL emission spectra of $Ca_xSr_{1-x}Al_2O_4:Tb^{3+}$ and $Ca_xSr_{1-x}Al_2O_4:Eu^{3+}$. All the phosphors were excited at 227 nm.

The calculated chromaticity coordinates of the white light emitting (A) Ca_xSr_{1-x} $Al_2O_4:Eu^{3+}$ are shown in Fig. 5. The chromaticity coordinates of the white light are x = 0.343, y = 0.325 and are very close to the chromaticity coordinates of standard white light (x = 0.333, y = 0.333) [22]. Also shown in the CIE diagram are the coordinates of red (B) $Ca_xSr_{1-x}Al_2O_4:Eu^{3+}$ and blue (C) $Ca_xSr_{1-x}Al_2O_4:Tb^{3+}$.

#169669 - $15.00 USD Received 1 Jun 2012; revised 17 Jun 2012; accepted 20 Jun 2012; published 21 Jun 2012

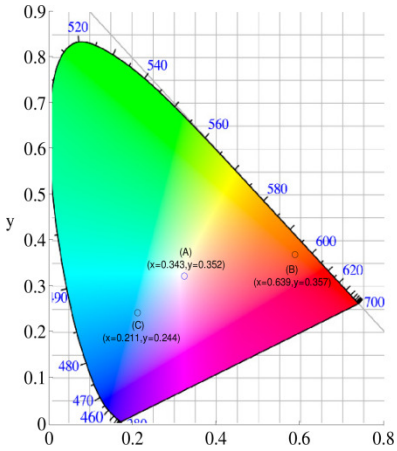

Fig. 5. The CIE diagram showing coordinates of white (A) $Ca_xSr_{1-x}Al_2O_4:Tb^{3+},Eu^{3+}$, red (B) $Ca_xSr_{1-x}Al_2O_4:Eu^{3+}$ and blue (C) $Ca_xSr_{1-x}Al_2O_4:Tb^{3+}$ phosphor.

4. Conclusion

In conclusion, a white light emitting $Ca_xSr_{x-1}Al_2O4:Tb^{3+},Eu^{3+}$ phosphor was prepared using the combustion method. The white light generated was a combination of simultaneous blue and green narrow line emission from Tb^{3+} and the red emission from Eu^{3+}. The production of the white light was shown to depend on the molar ratio of Ca^{2+} to Sr^{2+} in the host lattice, as well as the pump excitation wavelength. For example, the white light emission was observed when the sample with 0.3:0.7 mol ratio of Ca^{2+} to Sr^{2+} was excited at 227 nm. Our studies demonstrated that the material was excited through f→d transitions of Tb^{3+} and $O^{2-}\rightarrow Eu^{3+}$ charge transfer transitions. The f→d and $O^{2-}\rightarrow Eu^{3+}$ transitions occur simultaneously after excitation by photons of sufficiently high energy. The current study shows that the Ca_xSr_{x-1} $Al_2O_4:Tb^{3+},Eu^{3+}$ phosphor as a good material candidate for white LEDs and solid state lighting applications.

Acknowledgments

The authors would like to acknowledge the financial support from the cluster funds of the University of the Free State and the South African National Research Foundation.

#169669 - $15.00 USD Received 1 Jun 2012; revised 17 Jun 2012; accepted 20 Jun 2012; published 21 Jun 2012